DOI: 10.1002/cphc.200800734

Entangling Light in its Spatial Degrees of Freedom with Four-Wave Mixing in an Atomic Vapor

Vincent Boyer,*[a, b] Alberto M. Marino,[a] Raphael C. Pooser,[a] and Paul D. Lett[a]

The entanglement properties of two beams of light can reside in subtle correlations that exist in the unavoidable quantum fluctuations of their amplitudes and phases. Recent advances in the generation of nonclassical light with four-wave mixing in an atomic vapor have permitted the production and the observation of entanglement that is localized in almost arbitrary transverse regions of a pair of beams. These multi-spatial-mode entangled beams may prove useful for an array of applications ranging from noise-free imaging and improved position sensing to quantum information processing.

1. Introduction

When recorded with sensitive detectors, light reveals its quantum nature through the fluctuations in its observable properties, such as the amplitude and the phase. These fluctuations are the consequence of the Heisenberg uncertainty principle, and illustrate the probabilistic nature of quantum mechanics. Often referred to as shot noise, they were long regarded as a hindrance, limiting the accuracy of optical measurements and the signal-to-noise ratio of optical signals. This contrasts with classical electromagnetism, which does not account for these limitations and therefore may seem to describe a more perfect world. In the 1980s, progress in quantum optics showed that it is possible to get around the shot noise limit of a given observable by creating so-called squeezed states of light.[1]

More recently, it was realized that by allowing correlations to exist between the quantum fluctuations of distinct systems—they are then said to be entangled—quantum mechanics actually enables new possibilities beyond classical mechanics, such as fundamentally secure communications and increased information processing power.[2] Because of the unique properties of the electromagnetic field, such as fast and lossless propagation, quantum optics naturally finds its place in the new field of quantum information processing.

In conventional quantum optics, a beam of light is regarded as a single quantum object, described by the amplitude and the phase of its electric field. Quantum imaging brings the transverse spatial dimension into the problem and considers the fluctuations of the electric field at each point of the cross-section of the light beam: Various regions can have different quantum fluctuation properties.[3] This augments the capacity of the beam as a vector of quantum information and opens the door to improved optical measurements in imaging and positioning applications.

Herein, we review what it means for two beams of light to be squeezed or entangled, and we show how such beams can be created by four-wave mixing (4WM) in an alkali vapor. Advances in this technology have made it possible to directly observe entangled images,[4] that is, beams of light that display entanglement between arbitrary regions, or spatial optical modes, of their transverse profiles. We will conclude by presenting possible applications of these multi-spatial-mode beams to the detection of weakly absorptive objects, beam positioning and quantum information processing.

2. Entanglement of Light

The electric field of a monochromatic light wave of frequency ω can be classically described by an amplitude A and a phase ϕ or, equivalently, as the sum of a sine and a cosine which are referred to as the quadratures of the field, as in Equation (1):

$$E(t) \propto A\cos(\omega t + \phi) = X\cos\omega t + Y\sin\omega t \quad (1)$$

In quantum mechanics, non-commuting observables $\hat{X}$ and $\hat{Y}$, called the quadrature operators, correspond to the coefficients X and Y. They are much like the position and the momentum of a particle, and their commutator is given by Equation (2):[5]

$$\left[\hat{X}, \hat{Y}\right] = i/2 \quad (2)$$

From Equation (2), one can deduce a Heisenberg inequality on the uncertainty of these conjugate variables, as in Equation (3):

$$\left\langle \Delta\hat{X}^2 \right\rangle \left\langle \Delta\hat{Y}^2 \right\rangle \geq 1/16 \quad (3)$$

where $\left\langle \Delta\hat{X}^2 \right\rangle$ and $\left\langle \Delta\hat{Y}^2 \right\rangle$ denote the variances of the observables $\hat{X}$ and $\hat{Y}$, respectively. This indicates that one cannot measure simultaneously both quadratures of a light field with infin-

[a] Dr. V. Boyer, Dr. A. M. Marino, Dr. R. C. Pooser, Dr. P. D. Lett
Joint Quantum Institute
National Institute of Standards and Technology
University of Maryland, Gaithersburg, MD 20899 (USA)
[b] Dr. V. Boyer
MUARC
School of Physics and Astronomy, University of Birmingham
Edgbaston, Birmingham B15 2TT (United Kingdom)

ite precision. A special case of a minimum-uncertainty state is the coherent state, which is the output of a very quiet laser and the best approximation we have of a classical monochromatic wave. Its uncertainty is evenly shared between the conjugate variables so that Equation (4) can be written:

$$\langle \Delta \hat{X}^2 \rangle = \langle \Delta \hat{Y}^2 \rangle = 1/4 \quad (4)$$

When light is detected, this translates into noise on the electrical signal coming from the photodetectors. The uncertainty in Equation (4) is called the standard quantum limit (SQL), and is responsible for the shot noise level (Figure 1a). It is possible to prepare minimum-uncertainty states called squeezed coherent states for which one quadrature is less noisy than the SQL at the expense of the other quadrature, so that the equality in

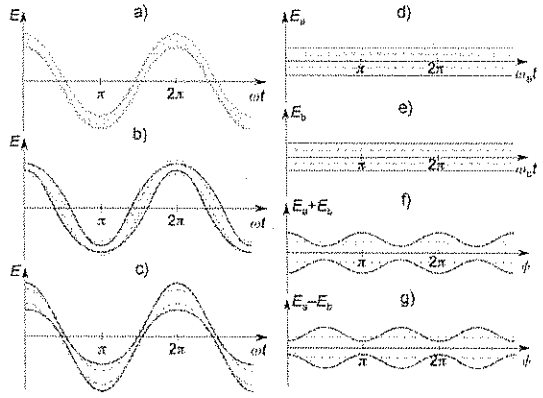

Figure 1. Phase evolution of the electric field for single-mode (b,c) and two-mode (d–g) squeezing. The blurring of the traces represents the quantum noise. a) Coherent state of frequency ω, whose noise is the SQL. The SQL is shown in the other figures with (·····). b) and c) State squeezed on the $\hat{X}$ and $\hat{Y}$ quadratures, respectively. For the choice of phase $\phi = 0$ in Equation (1), the state appears to be amplitude- and phase-squeezed, respectively. d) and e) Electric fields of the two-mode squeezed vacuum beams a and b. Their instant electric field is zero on average, but their fluctuations are above the SQL. The squeezing is visible on the f) sum and g) difference of their electric fields, which are alternatively below and above the SQL. The phase evolution corresponds to the joint quadratures $\hat{X}_-$ and $\hat{Y}_+$ being squeezed (with the choice of phase $\phi = 0$). The two modes do not necessarily have the same frequency ω_a and ω_b, but the sum and the difference are performed at equal running phases. Two-mode squeezing is easily generalized to beams with a nonzero instant electric field, as in (a–c).

Equation (3) is still realized. Figures 1 b,c show examples of squeezed light.

A more interesting case arises when one considers two beams of light (a and b), with respective quadratures ($\hat{X}_a$, $\hat{Y}_a$) and ($\hat{X}_b$, $\hat{Y}_b$). One can define two joint quadratures by mixing quadratures from the two beams and thus obtain Equations (5) and (6):

$$\hat{X}_- = (\hat{X}_a - \hat{X}_b)/\sqrt{2} \quad (5)$$

$$\hat{Y}_+ = (\hat{Y}_a + \hat{Y}_b)/\sqrt{2} \quad (6)$$

These new observables commute and therefore are not subject to a Heisenberg inequality. This means that it is possible to construct a minimum uncertainty two-mode squeezed state for which both joint quadratures are squeezed simultaneously, as shown in Equations (7) and (8):

$$\langle \Delta \hat{X}_-^2 \rangle < 1/4 \quad (7)$$

$$\langle \Delta \hat{Y}_+^2 \rangle < 1/4 \quad (8)$$

The corresponding conjugate operators $\hat{Y}_-$ and $\hat{X}_+$ have fluctuations larger than the SQL, so that again, the associated Heisenberg relations are exactly fulfilled: $\langle \Delta \hat{X}^2 \rangle \langle \Delta \hat{Y}^2 \rangle = \langle \Delta \hat{X}_+^2 \rangle \langle \Delta \hat{Y}_+^2 \rangle = 1/16$.

In this case, both beams are individually noisier than a coherent state of the same intensity in each of their two quadratures; however they exhibit strong correlations in their fluctuations, as shown in Figures 1 d–g. More specifically, measuring the $\hat{X}_a$ quadrature on beam a allows the $\hat{X}_b$ quadrature on beam b to be determined with an uncertainty smaller than its own SQL. The same goes for $\hat{Y}_a$ and $\hat{Y}_b$. Historically, this type of consideration has led to the Einstein–Podolsky–Rosen (EPR) paradox.[6,7] In apparent violation of the uncertainty principle, making a measurement on beam a makes it possible to deduce either $\hat{X}_b$ or $\hat{Y}_b$ to better than the SQL seemingly without disturbing beam b, as a local measurement would. In order to conserve the uncertainty principle, one has to admit that the reality of $\hat{X}_b$ and $\hat{Y}_b$ does not exist before the measurement is made on beam a. In other words, the two beams cannot be described independently, even if they are physically separated, and a measurement on one beam modifies the quantum state of the whole system, including beam b. We now know that this phenomenon, first described by Einstein as "spooky action at a distance", does not violate special relativity, that is, it does not allow the transmission of information faster than the speed of light.

By extension, the property of any quantum state in which the correlations between the beams apparently violate the uncertainty principle is called EPR entanglement. EPR-entangled states created in the laboratory tend to be statistical mixtures which are not minimum uncertainty states, but which display a level of squeezing on the $\hat{X}_-$ and the $\hat{Y}_+$ joint quadratures large enough to exhibit the EPR paradox.

Beams which are not EPR entangled can still be entangled according to a weaker entanglement criterion, called inseparability, which is fulfilled when $\langle \Delta \hat{X}_-^2 \rangle + \langle \Delta \hat{Y}_+^2 \rangle < 1/2$.[8,9] Two inseparable beams cannot be quantum mechanically described separately. Mathematically, it means that the total wavefunction $|\psi\rangle$ of the system cannot be factorized into a wavefunction for each subsystem as shown in Equation (9):

$$|\psi\rangle \neq |\psi_a\rangle \otimes |\psi_b\rangle \quad (9)$$

Obviously, a sufficient condition for inseparability is that both $\hat{X}_-$ and $\hat{Y}_+$ are squeezed. The concept of inseparability can be

extended to the case where the system is not in a pure state, but rather in a statistical mixture; the criterion is unchanged.

Entanglement of light was initially demonstrated for a pair of Gaussian-shaped optical modes, and the measured electric field was averaged over the full profile of the modes.[10] The goal in our experiments is to create entangled beams for which the quantum correlations can be seen locally in the transverse profile of the beams. Ideally, each point in beam *a* should be quantum-correlated to a unique point in beam *b*. In practice, a point in beam *a* is correlated to a region in beam *b*, called a coherence area, whose size is linked to the number of pairs of entangled modes present in the beams.

3. Four-Wave Mixing

Entangled beams of light can be created experimentally in nonlinear processes such as parametric down-conversion (PDC) and 4WM. In these processes, a certain number of beams, three in PDC and four in 4WM, interact in a nonlinear medium and energy is exchanged between the beams in such a way that both the total momentum and the total energy of the light are conserved. Our discussion focuses on nondegenerate 4WM[11] in a ^{85}Rb vapor,[12] but the physics is formally the same for PDC.

It is generally possible to choose a set of parameters (frequencies, directions of propagation, input intensities, etc.) so that an equal number of photons are transfered to two of the beams, usually called the probe and the conjugate, which are "twin beams". The other two beams are referred to as the pumps. In our case, there is a single beam playing the role of both pumps, and the probe and the conjugate form a very small angle with the direction *z* of the pump, as shown in Figure 2. In the limit of an energy transfer much smaller than the energy of the pump beam, the growth of the probe and conjugate electric fields E_a and E_b along the direction of propagation *z* is classically described by a cross-linear amplification, given by Equations (10) and (11):

$$\frac{\partial E_a}{\partial z} = \alpha E_b^* \tag{10}$$

$$\frac{\partial E_b^*}{\partial z} = \alpha' E_a \tag{11}$$

where α is a constant that depends on the pump power.

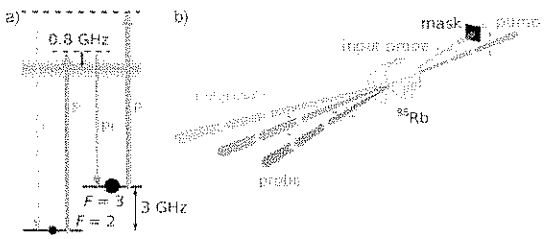

Figure 2. a) Energy diagram of the D1 line of ^{85}Rb showing the transitions involved in nondegenerate four-wave mixing. Starting from the ground state $F=3$, the atom is pumped into $F=2$ and then back into $F=3$. In the process, two pump (P) photons are absorbed and one probe (Pr) photon and one conjugate (C) photon are emitted. The width of the excited state represents the Doppler broadening. b) Setup geometry. A weak input probe beam intersects at a very small angle (< 10 mrad) with a strong pump beam in a ^{85}Rb vapor cell, and is amplified while a conjugate beam appears on the other side of the pump. The seeded optical mode (i.e., the bright profile) of the probe can be shaped with a mask placed in the beam. The output probe and conjugate are two-mode squeezed. When there is no input probe, the output is the two-mode squeezed vacuum described in Figure 1 (d–g). The double arrows indicate the relevant polarizations of the fields.

Quantum mechanically, this type of coupled propagation leads to a two-mode squeezed state for which the joint quadrature variances are $\langle \Delta \hat{X}_-^2 \rangle = \langle \Delta \hat{Y}_+^2 \rangle = e^{-2s}/4$ where $s = L|\alpha|$ and *L* is the length of the medium.[5] When the process is not seeded, that is, there is no input probe or conjugate, the output state is the two-mode squeezed vacuum described in Figures 1 d–g. The instantaneous electric fields of the output probe and conjugate are zero on average, but their fluctuations are quantum-correlated. When the process is seeded, that is, there is a weak input probe and no input conjugate, the power of the probe is amplified by a factor $G = \cosh^2 s$ while a conjugate beam with $G-1$ times the power of the input probe is created. The fluctuations of the probe and the conjugate are still quantum-correlated (although not perfectly).

The nondegenerate 4WM scheme presented in Figure 2 possesses a number of properties which are key to the successful generation of entangled beams and entangled images. First, the nonlinear gain *G* is high enough to ensure a large degree of squeezing of the joint quadratures. The gain is of the order of 5 for a 1.25 cm long cell heated to ≈100 °C and a pump power of ≈400 mW. Second, the scheme has been shown theoretically[13] and experimentally[14] to be largely free of competing processes such as fluorescence, Raman gain, and so forth, which add noise and can easily mask the squeezing. Finally, the 4WM naturally operates in a multi-spatial-mode regime. This means that more than one pair of optical modes for the probe and conjugate beams can be coupled in the medium.

This last point is an essential feature for the production of light fields entangled "region by region". The number of independent optical modes that can be coupled in the medium depends on geometrical parameters[15] and can be evaluated as follows. The smallest detail that can be imprinted on the twin beams in the far field, that is, far away from the nonlinear medium, is limited by diffraction off the finite-sized gain region. It is inversely proportional to the transverse size of the pump beam.

The number of these details that can fit (in the far field) in the probe and the conjugate beams is limited by the maximum possible divergence of the individual beams. In principle, the alignment and the collimation of the twin beams along the pump axis is enforced by the phase-matching condition, which expresses the conservation of the total momentum of the photons transferred from the pumps to the twin beams. However, the conservation of the longitudinal momentum is made uncertain (in the Heisenberg sense) for a gain region of finite length. The shorter the vapor cell, the more it can be violated and the more divergent the probe and conjugate modes can be. In our experiments, the total number of independent

modes, which is also the largest number of details that can be carried by an optical mode, is of the order of 10^2. This resolution allows the coupling of fairly detailed modes in the medium, as illustrated in Figure 3.

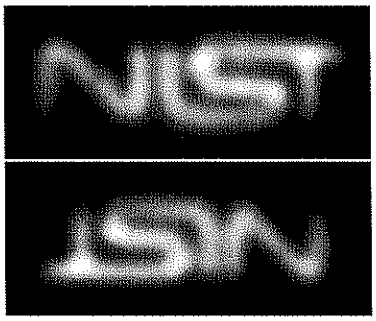

Figure 3. Amplification of a large and complex probe mode. The mode is generated by placing a mask in the input probe beam, as shown in Figure 2. The top image is the intensity profile of the output probe and the bottom image is the profile of the output conjugate created by the 4WM process.

The main restriction on the pairing of probe and conjugate modes is that they have to satisfy the phase-matching condition, specifically the conservation of the transverse momentum of light. As a result, they are essentially identical in shape and symmetric with respect to the pump axis.

Note that the exact number of independent modes would be given by the Schmidt decomposition. It consists of finding the "normal modes" of the system, that is, the pairs of probe and conjugate modes that are coupled in the medium by a defined coupling constant α or, to say it differently, modes that are amplified homogeneously in the medium (no distortion of the transverse profile). The "normal modes", or Schmidt modes, respect the symmetry of the problem, in particular the rotational invariance with respect to the pump axis, and are therefore eigenstates of the L_z angular momentum operator. An example of Schmidt decomposition is given by ref. [16] for PDC.

4. Observation of Entangled Images

The amplification of almost arbitrarily complex optical modes by the 4WM emphasizes the multi-spatial-mode nature of the process, at least for the mean intensity profiles of the probe and the conjugate. What remains to be shown is that this multi-spatial-mode character is present for the quantum fluctuations as well. In other words, for coupled regions in the output probe and conjugate, the quadratures of the corresponding fields should be entangled. As previously discussed, the entanglement of two beams does not depend on their mean intensity; in the following experiment we do not seed the 4WM process, therefore producing a two-mode squeezed vacuum.

The quadratures of a light field can be measured with a homodyne detector (HD).[17] It consists of a strong beam of identical frequency to the signal, called the local oscillator (LO), which interferes with the field to be analyzed. The amplitude of the interference, recorded by a balanced photodetector, is a direct measure of the generalized quadrature $\hat{X}_\theta = \hat{X}\cos\theta + \hat{Y}\sin\theta$, where θ is the phase of the LO relative to the phase of the analyzed field. By scanning θ, one can successively measure the $\hat{X}$ and the $\hat{Y}$ quadratures. As shown in Figure 4,

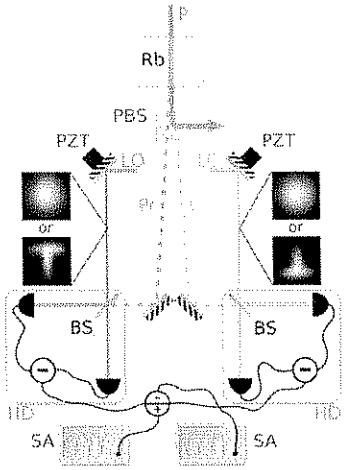

Figure 4. Experimental setup for the production and the analysis of entangled images. The pump (P) in the vapor cell creates a two-mode squeezed vacuum represented by the dashed lines. The twin beams are measured with homodyne detectors. Each homodyne detector involves a local oscillator and produces a photocurrent proportional to the generalized quadrature $\hat{X}_\theta$, where θ is the phase difference between the LO and the analyzed field. It is chosen to be the same for both HDs and is set by the piezoelectric transducers (PZT). The generation of the LOs is not shown. The spectrum analyzers (SA) measure the fluctuations of the sum and the difference of the generalized quadratures. The optical modes analyzed in the HDs are defined by the shape of the LOs. As shown in the small pictures, we tested two different kinds of intensity profile, a Gaussian mode and a "T"-shaped mode. As long as the LO profiles are matched, i.e., they are identical and rotated by 180° with respect to each other, squeezing on $\hat{X}_-$ and $\hat{Y}_+$ is observed.

we record the quadratures of both the probe and conjugate, and we form the sum and the difference of the photocurrents. The fluctuations of the sum and difference signals are then measured with radio frequency spectrum analyzers. When the phases of the LOs are both $\theta = 0$ or π, the difference signal is proportional to $\hat{X}_-$ and the spectrum analyzer measures the variance $\langle \Delta\hat{X}_-^2 \rangle$. When the phases of the LOs are both $\theta = \pm\pi/2$, the sum signal is proportional to Y_+ and the spectrum analyzer measures the variance $\langle \Delta\hat{Y}_+^2 \rangle$.

Experimentally, the phases of the LOs are scanned synchronously in such a way that they are equal at all times. The measured noises of the sum and difference signals, shown in Figure 5, follow the oscillations seen on the amplitude of the fluctuations in Figures 1 f,g. The fact that the noise traces alternately go under the SQL proves that the output state is inseparable. The level of squeezing (noise more than 3 dB below the SQL) is also enough to infer that the probe and the conjugate are EPR entangled.

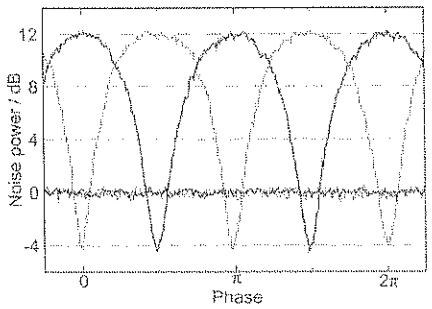

Figure 5. Noise levels of the sum (——) and the difference (·····) of the generalized quadratures as the phase θ of the homodyne detectors is scanned. The reference level (0 dB) is set to the SQL. The SQL is determined by blocking the input of the HDs, that is to say by injecting vacuum coherent states. The dips of the noise traces show that the variances $\langle \Delta \hat{X}_-^2 \rangle$ and $\langle \Delta \hat{Y}_+^2 \rangle$ are below the SQL. This data is for Gaussian-shaped LOs, but "T"-shaped LOs also display more than 3 dB of squeezing.

The crucial point here is that the regions of the entangled output beams analyzed by the HDs correspond to the optical modes (the shapes) of the LOs. It is therefore straightforward to observe the multimode character of the entanglement by varying the modes of the LOs and checking that the squeezing on the joint quadratures is conserved. This is what we see (Figure 4), as long as the chosen modes are symmetric with respect to the pump axis and are contained in the spatial resolution of the 4WM. The number of pairs of entangled modes is equal to the number of orthogonal LO modes that can be used to record some squeezing, and is equal to the number of independent modes calculated in the previous section ($\approx 10^2$).[4]

This behavior is in stark contrast with what is observed for single-spatial mode entanglement, which is what is typically obtained from an optical parametric oscillator (OPO) below threshold.[10] In this case, the output modes of the entangled beams are uniquely defined by an optical cavity, and choosing LO modes which do not match the cavity mode results in a severe reduction in the measured squeezing of the joint quadratures. Multimode operation in an OPO is possible, but the cavity has to be carefully tuned to be transversely degenerate.[18]

5. Applications

We collect here some of the most promising ideas for the application of multi-spatial-mode entanglement. It is fair to say that since its first demonstration in 1985, squeezed light has not found its way to practical applications, except possibly for the impending use of single-mode squeezing in gravitational wave interferometers.[19] Multi-spatial-mode-squeezed beams could change this state of the field.

Most of the applications aiming to improve measurements beyond the shot noise limit rely on the squeezing of a single joint quadrature, so entanglement is not strictly required.

A first application of quantum-correlated beams is the imaging of weakly absorptive objects. The measurement of the absorption of a beam of light propagating through an almost transparent medium is limited by the quantum fluctuations on the amplitude of the electric field, which translate into fluctuations on the optical power. By choosing the (arbitrary) phase ϕ in Eq. (1) equal to zero, we make $\hat{X}$ the amplitude quadrature. It is possible to get around the SQL by using beams whose joint quadrature $\hat{X}_-$ is squeezed, which is what is generated by the 4WM when the probe is seeded with a coherent state and the conjugate with the vacuum. The squeezing on the power difference can be measured with a balanced photodetector. Since the power-difference noise is below the SQL, it is possible to measure a loss of power on one of the beams smaller than the SQL, and therefore to detect a very small absorption.[20] With multi-spatial-mode twin beams, one can extend that idea to the imaging of a weakly absorptive object.[21] Using a camera or an array of photodiodes to record the distribution of light in the beam profiles, one can form the absorption image of the object with less noise than if the object were to be illuminated with a coherent state.

A related issue is beam positioning. It is an important component for applications such as the measurement of the displacement of the tip of an atomic force microscope, the detection of the motion of a bead trapped in an optical tweezer[22] or mirage spectroscopy.[23] The position of a beam of light is defined as the position of the center of mass of its intensity profile, and can be measured by a camera or a quadrant detector. It is a classically well-defined quantity, but intensity quantum fluctuations randomly distributed on the beam profile make the position of even a quiet laser beam uncertain, therefore introducing an SQL on the position of the beam. Because multi-spatial-mode twin beams have the same localized intensity fluctuations in their profiles, one can measure a deflection of one of the twin beams smaller than the SQL by subtracting the position fluctuations of the other beam.

Finally, entangled light is likely to find good use in quantum information processing because it is an efficient way to transfer entanglement, an essential ingredient of quantum algorithms, between physical locations. The 4WM described here is an economical way of producing a large number ($\approx 10^2$) of pairs of entangled modes at once. The challenge to make this solution a practical one is to separate the different spatial modes in order to analyze them simultaneously and to manipulate them individually.

6. Conclusions

Nondegenerate four-wave mixing in atomic vapors has revealed itself to be a tool of choice for the generation of spatially entangled light fields, and should certainly contribute to the maturation of the field of quantum imaging. The naturally multi-spatial-mode operation of 4WM opens intriguing new possibilities for the production of complex quantum states. For instance, it would be possible to replace the point-to-point correlations between the profiles of the twin beams with a more complex geometrical relationship by tailoring the spatial mode of the pump beam. As an example, a Laguerre–Gauss pump beam creates a point-to-circle correspondence between

the probe and the conjugate.[24] Combined with the flexibility offered by the spatial manipulation of the light, complex spatial entanglement may prove useful for quantum information science.

Acknowledgements

R. C. P. is supported under a grant from the Intelligence Community Postdoctoral Program.

Keywords: absorption imaging · atomic vapors · entangled beams · four-wave mixing · rubidium

[1] R. E. Slusher, L. W. Hollberg, B. Yurke, J. C. Mertz, and J. F. Valley, *Phys. Rev. Lett.* **1985**, *55*, 2409.
[2] M. A. Nielsen and I. L. Chuang, *Quantum Computation and Quantum Information*, Cambridge University Press, Cambridge, **2000**.
[3] M. I. Kolobov (Ed.), *Quantum imaging*, Springer, New York, **2007**.
[4] V Boyer, A. M. Marino, R. C. Pooser, and P. D. Lett, *Science* **2008**, *321*, 544–547.
[5] R. Loudon, *The Quantum Theory of Light (3rd Edition)*, Oxford University Press, Oxford, **2000**.
[6] A. Einstein, B. Podolsky, and N. Rosen, *Phys. Rev.* **1935**, *47*, 777.
[7] M. D. Reid, *Phys. Rev. A* **1989**, *40*, 913.
[8] L.-M. Duan, G. Giedke, J. I. Cirac, and P. Zoller, *Phys. Rev. Lett.* **2000**, *84*, 2722.
[9] R. Simon, *Phys. Rev. Lett.* **2000**, *84*, 2726.
[10] Z. Y. Ou, S. F. Pereira, H. J. Kimble, and K. C. Peng, *Phys. Rev. Lett.* **1992**, *68*, 3663.
[11] P. R. Hemmer, D. P. Katz, J. Donoghue, M. Cronin-Golomb, M. S. Shahriar, and P. Kumar, *Opt. Lett.* **1995**, *20*, 982,.
[12] C. F. McCormick, V. Boyer, E. Arimondo, and P. D. Lett, *Opt. Lett.* **2007**, *32*, 178–180.
[13] M. D. Lukin, P. R. Hemmer, and M. O. Scully, *Adv. Atom Mol. Opt. Phy.* **2000**, *42*, 347–386.
[14] C. F. McCormick, A. M. Marino, V. Boyer, and P. D. Lett, *Phys. Rev. A* **2008**, *78*, 043816.
[15] P. Kumar and M. I. Kolobov, *Opt. Comm.* **1994**, *104*, 374–378.
[16] C. K. Law and J. H. Eberly, *Phys. Rev. Lett.* **2004**, *92*, 127903.
[17] H. P. Yuen and V. W. S. Chan, *Opt. Lett.* **1983**, *8*, 177–179.
[18] L. Lopez, N. Treps, B. Chalopin, C. Fabre, and A. Maître, *Phys. Rev. Lett.* **2008**, *100*, 013604.
[19] K. Goda, O. Miyakawa, E. E. Mikhailov, S. Saraf, R. Adhikari, K. McKenzie, R. Ward, S. Vass, A. J. Weinstein, and N. Mavalvala, *Nat. Phys.* **2008**, *4*, 472–476.
[20] P. R. Tapster, S. F. Seward, and J. G. Rarity, *Phys. Rev. A* **1991**, *44*, 3266.
[21] E. Brambilla, L. Caspani, O. Jedrkiewicz, L. A. Lugiato, and A. Gatti, *Phys. Rev. A* **2008**, *77*, 053807–11.
[22] K. Visscher, S. P. Gross, and S. M. Block, *IEEE J. Sel. Top. Quantum Electron.* **1996**, *2*, 1066–1076.
[23] A. C. Boccara, D. Fournier, and J. Badoz, *Appl. Phys. Lett.* **1980**, *36*, 130–132.
[24] A. M. Marino, V. Boyer, R. C. Pooser, P. D. Lett, K. Lemons, and K. M. Jones, *Phys. Rev. Lett.* **2008**, *101*, 093602–4.

Received: November 6, 2008
Published online on February 18, 2009

